AMERICAN SOCIETY FOR MICROBIOLOGY | Antimicrobial Agents and Chemotherapy®

EXPERIMENTAL THERAPEUTICS

The Antimicrobial Peptide MK58911-NH_2 Acts on Planktonic, Biofilm, and Intramacrophage Cells of *Cryptococcus neoformans*

Junya de Lacorte Singulani,[a] Lariane Teodoro Oliveira,[a] Marina Dorisse Ramos,[a] Nathália Ferreira Fregonezi,[a] Paulo César Gomes,[a] Mariana Cristina Galeane,[a] Mario Sergio Palma,[b] Ana Marisa Fusco Almeida,[a] Maria José Soares Mendes Giannini[a]

[a]Department of Clinical Analysis, School of Pharmaceutical Sciences, São Paulo State University-UNESP, Araraquara, Brazil
[b]Department of Basic and Applied Biology, Institute of Biosciences, São Paulo State University-UNESP, Rio Claro, Brazil

ABSTRACT Cryptococcosis is associated with high rates of morbidity and mortality, especially in AIDS patients. Its treatment is carried out by combining amphotericin B and azoles or flucytosine, which causes unavoidable toxicity issues in the host. Thus, the urgency in obtaining new antifungals drives the search for antimicrobial peptides (AMPs). This study aimed to extend the understanding of the mechanism of action of an AMP analog from wasp peptide toxins, MK58911-NH_2, on *Cryptococcus neoformans*. We also evaluated if MK58911-NH_2 can act on cryptococcal cells in macrophages, biofilms, and an immersion zebrafish model of infection. Finally, we investigated the structure-antifungal action and the toxicity relationship of MK58911-NH_2 fragments and a derivative of this peptide (MH58911-NH_2). The results demonstrated that MK58911-NH_2 did not alter the fluorescence intensity of the cell wall-binding dye calcofluor white or the capsule-binding dye 18b7 antibody-fluorescein isothiocyanate (FITC) in *C. neoformans* but rather reduced the number and size of fungal cells. This activity reduced the fungal burden of *C. neoformans* in both macrophages and zebrafish embryos as well as within biofilms. Three fragments of the MK58911-NH_2 peptide showed no activity against *Cryptococcus* and not toxicity in lung cells. The derivative peptide MH58911-NH_2, in which the lysine residues of MK58911-NH_2 were replaced by histidines, reduced the activity against extracellular and intracellular *C. neoformans*. On the other hand, it was active against biofilms and showed reduced toxicity. In summary, these results showed that peptide MK58911-NH_2 could be a promising agent against cryptococcosis. This work also opens a perspective for the verification of the antifungal activity of other derivatives.

KEYWORDS antimicrobial peptide, systemic mycoses, antifungal activity, cryptococcosis, biofilm, nonconventional animal models, intramacrophage activity, *Cryptococcus neoformans*, antifungal agents, mechanisms of action, systemic fungi

In recent years, there has been a substantial increase in the incidence of systemic mycosis due to both medical advances and the rise of immunosuppressive diseases. Cryptococcosis, for example, was estimated to be responsible for more than 200,000 incident cases worldwide in 2014 and 15% of AIDS-related deaths (1). Its etiological agents are found in environments contaminated by feces of pigeons and other birds (*Cryptococcus neoformans*) or by the decomposition of wood and other plant materials (*Cryptococcus gattii*) (2).

The first site of infection of *Cryptococcus* spp. is the lung, where alveolar macrophages are the first immune cells to encounter the fungus. In this organ, either the host's immune response controls the infection or the fungus successfully escapes this response and, without treatment, spreads systemically, with fatal consequences. In order to disseminate within the host, *Cryptococcus* spp. can proliferate, transfer, and escape from macrophages lytically or nonlytically (via vomocytosis) (3–5). This process is believed to strongly

Citation Singulani JDL, Oliveira LT, Ramos MD, Fregonezi NF, Gomes PC, Galeane MC, Palma MS, Fusco Almeida AM, Mendes Giannini MJS. 2021. The antimicrobial peptide MK58911-NH_2 acts on planktonic, biofilm, and intramacrophage cells of *Cryptococcus neoformans*. Antimicrob Agents Chemother 65: e00904-21. https://doi.org/10.1128/AAC.00904-21.

Address correspondence to Maria José Soares Mendes Giannini, gianninimj@gmail.com, or Junya de Lacorte Singulani, junyadelacorte@yahoo.com.br.

Received 2 May 2021
Returned for modification 5 June 2021
Accepted 19 August 2021
Accepted manuscript posted online 13 September 2021
Published 17 November 2021

influence the migration of *C. neoformans* and *C. gattii* to the central nervous system, where they cause cryptococcal meningitis in immunocompromised patients, especially those in advanced stages of AIDS; patients on immunosuppressive therapy; or patients with hematological malignancies (6–8).

Although rapid antifungal therapy is relatively effective, there is a limited number of classes of these drugs. Cryptococcosis is usually treated with fluconazole, while severe cases, including cryptococcal meningitis, are treated with amphotericin B together with 5-fluorocytosine or fluconazole (9). However, many antifungal agents display side effects and drug-drug interactions (10). Another problem is increasing fungal species with natural or acquired resistance to currently available antifungal drugs. For example, *C. neoformans* has intrinsic resistance to a newer class of antifungal agents, the echinocandins (11, 12). In addition, *Cryptococcus* spp. can colonize and form biofilms on medical devices such as ventriculoatrial shunt catheters, prosthetic valves, and prostheses, representing a significant health concern due to their resistance to antifungal treatment (13). Thus, the search for new antifungal targets and more efficient and less toxic drugs has been ongoing.

Antimicrobial peptides (AMPs) are important molecules that act as the first line of defense to combat pathogens in many organisms and are attractive alternatives to antifungal drugs. Some AMPs have multiple targets in microorganisms, which reduces the chances of resistance development, while others are more specific in their mechanism of action, acting mainly on the bacterial and/or fungal membrane (14, 15). In addition, their applications are also being investigated as promising antibiofilm drugs (16, 17).

Here, we explore a social wasp venom-derived AMP, which belongs to the mastoparan class, as a promising antifungal agent. Previous studies with mastoparan peptides revealed their activity against Gram-positive and Gram-negative bacteria through interaction with membranes (18, 19). Furthermore, we demonstrate that the mastoparan derivative MK58911-NH_2 causes membrane damage in *C. neoformans* cells and has *in vivo* antifungal efficacy in the *Galleria mellonella* wax moth model (20).

Here, we provide more detailed information about the mode of action of MK58911-NH_2 and verify its efficacy against *C. neoformans* in macrophages and biofilms. We also evaluate if fragments from MK58911-NH_2 and its derivative MH58911-NH_2, in which the lysine residues of MK58911-NH_2 were replaced by histidine residues, still present antifungal activity and toxicity. For *in vivo* assays, we used zebrafish embryos, which have been applied extensively for toxicological studies in drug development (21) and more recently as a model for fungal infections, including *Cryptococcus* spp. (22–25).

RESULTS

The intensity of calcofluor white fluorescence of *C. neoformans* cell walls did not reveal a change in the chitin content upon exposure to MK58911-NH_2 (Fig. 1D to G) compared to the control (Fig. 1A and G) or cells treated with amphotericin B (Fig. 1B and G) and fluconazole (Fig. 1C and G) after 4 h of treatment. On the other hand, the number of cells in the control group, 6.2×10^6 (Fig. 1A and H), was significantly reduced to 1.4×10^6 cells ($P < 0.05$) (Fig. 1D to F and H) in the group incubated in the presence of MK58911-NH_2.

Staining the capsule with India ink revealed that MK58911-NH_2 did not change the diameter of this structure compared to the untreated control group (Fig. 2A, B, and G). However, the peptide reduced the total and body diameters (without capsule) of the fungal cell ($P < 0.05$) (Fig. 2A, B, E, and F). Staining *C. neoformans* with antibody 18b7-fluorescein isothiocyanate (FITC) demonstrated no difference in the mean fluorescence intensities between the capsules of *C. neoformans* cells treated with the peptide and those of the control group (Fig. 2C, D, and H).

The peptide action was also verified in zebrafish embryos exposed to a fungal suspension of *C. neoformans* at 1×10^6 cells/ml for 24 h using an immersion model.

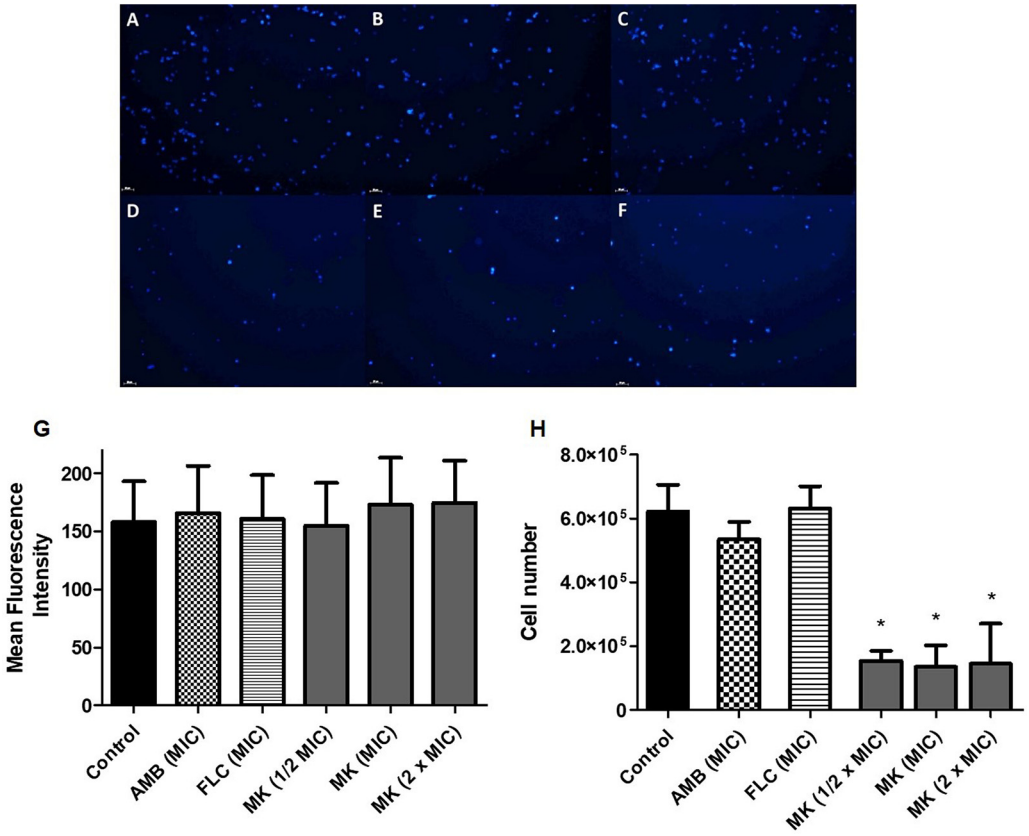

FIG 1 *C. neoformans* cells exposed to the peptide for 4 h and marked with calcofluor white. (A) Control; (B) amphotericin B (AMB) at the MIC; (C) fluconazole (FLC) at the MIC; (D to F) peptide MK58911-NH_2 (MK) at 1/2× MIC, the MIC, and 2× MIC; (G) average fluorescence intensity per cell; (H) number of cells. Data represent the means (± standard deviations [SD]) from three independent experiments. *, $P < 0.05$ compared to the control.

During this period, fungal cells adhered to the embryos' chorion, for which the images of cells (labeled with calcofluor white) were acquired 4 h after exposure to the fungus (Fig. 3A to C). Exposure to treatments with MK58911-NH_2 or the control drug amphotericin B for 24 h resulted in a significant reduction in CFU compared to the untreated control (Fig. 3D). In contrast, the drug fluconazole did not reduce the fungal burden of the embryos' chorion. All embryos survived treatment with MK58911-NH_2 or antifungal drugs.

The peptide MK58911-NH_2 can also be an excellent model for designing analog peptides as novel antifungal agents. In this aspect, four derivative peptides from MK58911-NH_2 were synthesized and used to analyze antifungal activity and cytotoxicity. In one of these peptides, the lysine residues were replaced by histidine residues, while the other amino acid residues were maintained in the same positions as those observed in MK58911-NH_2; this peptide was designated MH58911-NH_2 (Table 1). Meanwhile, the other three peptides corresponded to shorter sequences of the MK58911-NH_2 peptide to verify which fragments could be responsible for the activity. Furthermore, to establish a correlation between the structural features of the peptides and the biological activities, we simulated the secondary structures of each peptide using the PEP2D algorithm as a bioinformatic tool (26). The results are shown in Table 1, which reveals that MK58911-NH_2 presents 57.14% helices and 42.86% coils; meanwhile, MH58911-NH_2 presents 50% helices and 50% coils. The simulation for MK58911(4–11)-OH revealed 37.50% helices and 62.50% coils. The algorithm calculated that MK58911(1–7)-OH presents one element of the sheet, while MK58911(8–14)-NH_2 has two of these elements of secondary structure, covering 14.29% and 28.57% of their sequences, respectively. The remaining

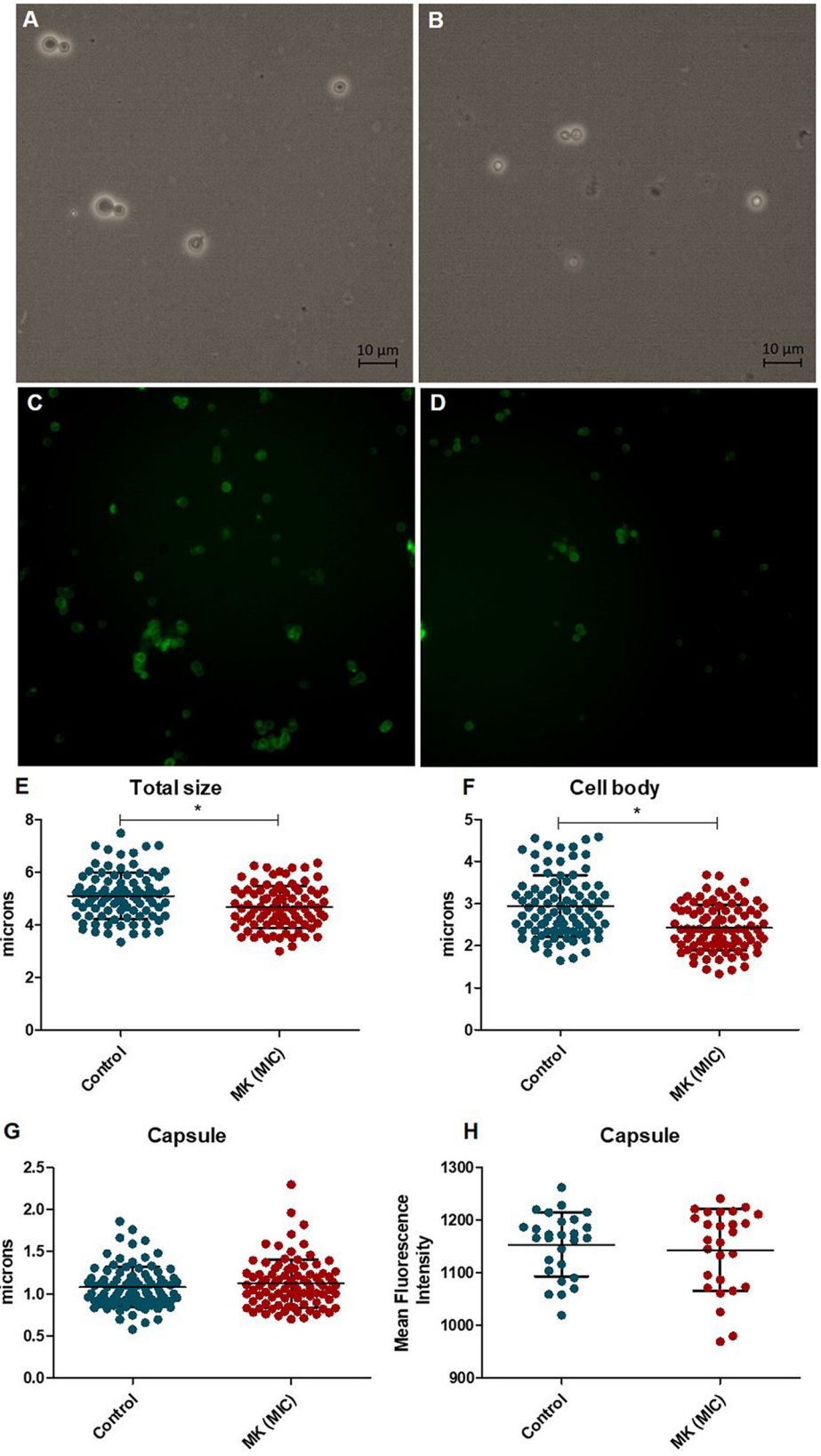

FIG 2 *C. neoformans* cells exposed to the peptide for 4 h and marked with India ink (A, B, and E to G) or antibody 18b7 (C, D, and H). (A and C) control; (B and D) peptide MK58911-NH_2 (MK) at the MIC; (E) total cell diameter; (F) diameter of the cell body (without capsule); (G) diameter of the capsule; (H) average fluorescence intensity per cell. Data represent the means (±SD) from three independent experiments. *, $P < 0.05$ compared to the control.

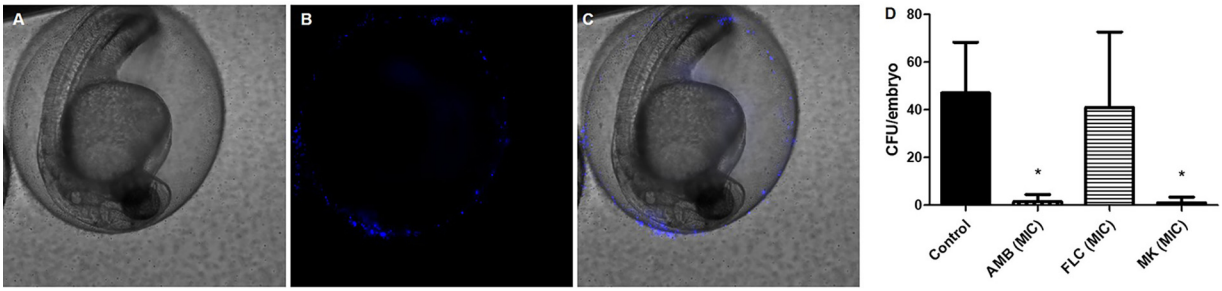

FIG 3 Representative images of zebrafish embryos exposed to a fungal suspension (1×10^6 cells/ml) of *C. neoformans*. (A) Bright-field image; (B) fungal cells labeled with calcofluor white; (C) overlay of images; (D) effect on the fungal load in embryos infected and exposed to treatments with MK58911-NH_2 (MK), amphotericin B (AMB), and fluconazole (FLC) at the MIC for 24 h. Data represent the means (±SD) from two independent experiments. *, $P < 0.05$ compared to the control.

structures of these peptides are constituted of coils. However, *in vitro* assays revealed that none of the peptide fragments or derivatives showed activity against *Cryptococcus* spp. and toxicity to pulmonary fibroblasts (MRC5 cells) at the evaluated concentrations (Table 2).

The determination of the activity of the peptides MK58911-NH_2 and MH58911-NH_2 against *C. neoformans* within macrophages and biofilms and their comparison were also performed. The J774 macrophage line was infected with *C. neoformans* and then exposed to treatments with the peptides and the control drugs amphotericin B and fluconazole. As shown in Fig. 4A, the peptide MK58911-NH_2, amphotericin B, and fluconazole led to a significant reduction ($P < 0.05$) in the intramacrophagic fungal burden, with averages of 2.0×10^3, 1.1×10^3, and 1.8×10^3 CFU/well, respectively, compared to the control (4.5×10^3 CFU/well). However, the cells treated with MH58911-NH_2 showed an average CFU value (4.9×10^3 CFU/well) similar to that of the control. The cytotoxicity of both peptides was also verified with macrophages, and MH58911-NH_2 was shown to be less toxic, with a 50% inhibitory concentration (IC_{50}) of >250 μg/ml, than MK58911-NH_2, with an IC_{50} of 62.50 μg/ml (Fig. 4B).

To test activity against biofilms of *C. neoformans*, treatments were carried out at 0 h (the beginning of biofilm formation) and on fully formed biofilms at 48 h. Both peptides

TABLE 1 Amino acid sequences and prediction of secondary structures of the peptides tested in the present study[a]

Peptide	Sequence	Secondary structure	Helix [H] (%)	Sheet [E] (%)	Coil [C] (%)
MK58911- NH2	INWLKIAKKVKGML-NH2	Conf. CCCHHHHHHHHCCC	57.14	0.00	42.86
MH58911- NH2	INWLHIAHHVHGML-NH2	Conf. CCCHHHHHHHHCCC	50.00	0.00	50.0
MK58911 (1-7)-OH	INWLKIA-OH	Conf. CCCCECC	0.00	14.29	85.71
MK58911 (8-14)-NH2	KKVKGML-NH2	CCCECEC	0.00	28.57	71.43
MK58911 (4-11)-OH	LKIAKKVK-OH	Conf. CCHHHCCC	37.50	0.00	62.50

[a]Prediction of the secondary structures of the peptides was based on the PEP2D algorithm (https://webs.iiitd.edu.in/raghava/pep2d/submit.html). The structural elements are represented as follows: helix, pink cylinders; sheet, yellow triangles; coil, black lines.

TABLE 2 Activity against *Cryptococcus* species and toxicity in pulmonary fibroblasts (MRC5 cells) of MK58911-NH_2 peptide derivatives[a]

Peptide or drug	*C. neoformans* MIC (μg/ml)	*C. gattii* MIC (μg/ml)	MRC5 IC_{50} (μg/ml)
MK58911-NH_2	31.25	15.63	>500
MK58911(1–7)-OH	>250	>250	>500
MK58911(8–14)-NH2	>250	>250	>500
MK58911(4–11)-OH	>250	>250	>500
MH58911-NH_2	>250	>250	>500
Amphotericin B	0.125	0.125	
Fluconazole	1	8	

[a]IC_{50}, 50% inhibitory concentration.

decreased the metabolic activity of biofilms in a concentration-dependent manner, where values of ≥250 μg/ml for MK58911-NH_2 and ≥500 μg/ml for MH58911-NH_2 led to a reduction of at least 50% of the metabolic activity of both nascent (Fig. 5A) and mature (Fig. 5B) biofilms.

DISCUSSION

Considering the inferior status of currently available antifungal drugs, new treatment options for cryptococcosis are needed. In this respect, studies from several groups have attempted to address the use of AMPs as antifungal agents (15). Currently, more than 3,000 AMPs are known; however, the mechanisms of action are characterized for only a reduced number of these peptides (27). The interaction of the AMPs with the fungi generally targets the fungal cell membrane and/or cell wall; however, some peptides can interact with intracellular targets (28). We previously demonstrated the *in vitro* and *in vivo* activity of the MK58911-NH_2 peptide against *Cryptococcus* and its mechanism of action on the fungal membrane (20). Here, we verified the possible action of peptides on other cell structures of *C. neoformans*.

The cryptococcal cell wall comprises glucans (more β-1,6- than β-1,3-glucan), chitin, chitosan, mannoproteins, and glycosylphosphatidylinositol (GPI)-anchored proteins. Collectively, these components maintain the shape and rigidity of the cell and are essential for infection (29, 30). The polysaccharide capsule is anchored to the outer layer of the cell wall and is considered the main virulence factor of *Cryptococcus* spp. (29–31). The capsule of this yeast is composed of glucuronoxylomannan (GXM), galactoxylomannan (GalXM), and mannoproteins and is important for protection from desiccation, radiation, and phagocytosis (23, 31–34). All elements of the fungal cell wall and capsule can be excellent targets for antifungal compounds. However, our peptide MK58911-NH_2 did not alter the fluorescence intensity of calcofluor white (chitin-binding dye) and 18b7-FITC

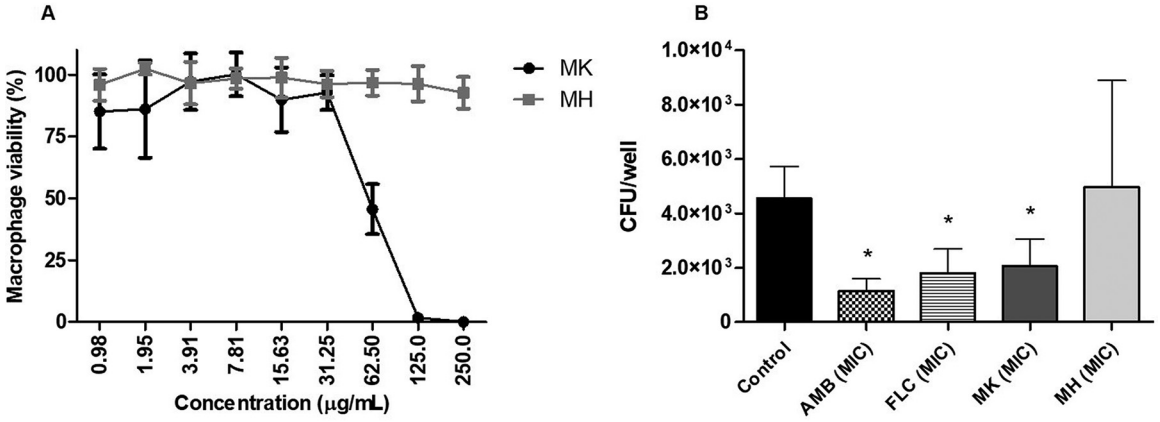

FIG 4 Activity of peptides MK58911-NH_2 and MH58911-NH_2 against intramacrophage *C. neoformans* (A) and on the viability of J774 macrophages (B). AMB, amphotericin B; FLC, fluconazole. Data represent the means (±SD) from three independent experiments. *, $P < 0.05$ compared to the control.

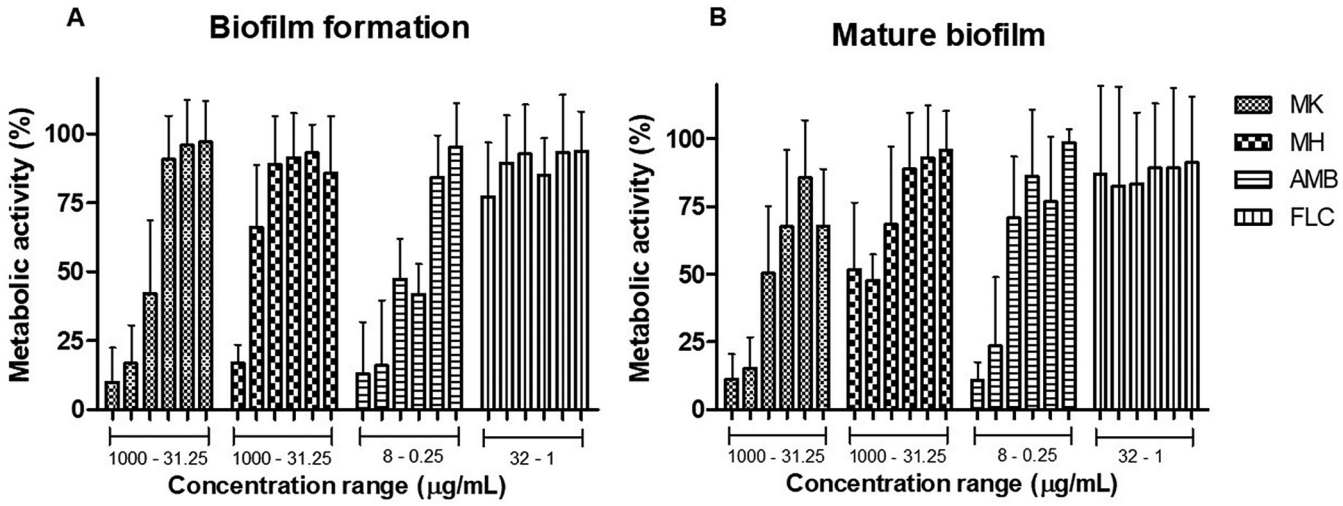

FIG 5 Activity of peptides MK58911-NH_2 (MK) and MH58911-NH_2 (MH) on biofilm formation at 0 h (A) and mature biofilm at 48 h (B) of *C. neoformans*. AMB, amphotericin B; FLC, fluconazole. Data represent the means (±SD) from three independent experiments. *, $P < 0.05$ compared to the control.

(GXM-binding antibody) staining of the cell wall and capsule, respectively, in *C. neoformans*; on the other hand, this peptide reduced cell size and led to fungal death, which might be a result of cell membrane damage (20, 35, 36). The peptides from the mastoparan class such as MK58911-NH_2 seem to accumulate on the membrane of microorganisms in a carpet-like manner, attracted by electrostatic interactions, and consequently, the membranes are disrupted (18, 37).

We next assessed the effect of MK58911-NH_2 on intramacrophage *C. neoformans*. Although most studies have focused on compounds that act on extracellular cryptococci, the action on intracellular fungi is very important since the replication and spread of the host's fungi are partially determined by macrophage-pathogen interactions (38). In our study, the peptide MK58911-NH_2 reduced the intramacrophage fungal burden, in addition to exhibiting a direct effect on the fungus, as previously described (20).

Due to the pronounced risk of antifungal resistance associated with biofilm formation, the effect of MK58911-NH_2 on the initial stage and mature biofilms was also evaluated. The resistance of fungal biofilms involves several features such as the overexpression of drug resistance genes and impairment of drug penetration due to the extracellular matrix (39). This study produced results that corroborate the findings of Martinez and Casadevall (13), which demonstrated that *C. neoformans* biofilms are resistant to fluconazole. However, the formation of *C. neoformans* biofilms can be prevented at concentrations of >0.5 μg/ml, and mature biofilms can be inhibited at concentrations of >2 μg/ml by high doses of amphotericin B. MK58911-NH_2 presented an antifungal effect on different phases of the biofilm process at formation and mature biofilms. Furthermore, higher concentrations than those in planktonic cells were required for this peptide action (8× MIC), which are lower concentrations than expected for antifungal agents (100× to 1,000× MIC) according to previous studies (39, 40). Similar to MK58911-NH_2, another peptide from the mastoparan class, polybia-MPI, caused membrane damage and inhibition of biofilm formation of *Candida* species (41).

After *in vitro* assays, we used an immersion model of zebrafish embryos for *C. neoformans* adhesion and evaluation of peptide antifungal efficacy. Treatment with MK58911-NH_2 resulted in a significant reduction in the burden of fungi adhered to the chorion of the embryos. The noninvasive zebrafish embryo bath immersion model was performed using *Candida albicans*, in which the medium used, the inoculum concentration, and the ideal incubation time for the experiment were standardized (22). Subsequently, it was demonstrated that the adhered fungal cells form biofilms on the embryos' chorion (42). Although we verified that a smaller number of *C. neoformans* cells adhered to the embryos than that of *C. albicans* cells demonstrated in previous

studies (22, 42), the structure observed in our analysis is biofilm-like, with apparent agglomerate and extracellular matrix formation at 24 h postinfection (data not shown). Another result that corroborates this fact is that fluconazole did not reduce the fungal burden in the embryos, which also happens when this drug is tested against *C. neoformans* biofilms *in vitro* (13). However, further studies are needed to confirm this suggestion.

Finally, we tested some fragments of the peptide MK58911-NH_2 to try to find out which portion of the molecule is responsible for its antifungal activity. A derivative with the same sequence as that of MK58911-NH_2 but in which the lysine residues have been replaced by histidine residues (MH58911-NH_2) was also assayed. In an attempt to correlate the structural features of the MK and MH series of peptides with their biological activities, the secondary structures of the five peptides used in the present study were simulated using a bioinformatics approach. AMPs are typically constituted of up to 54 amino acid residues in their sequences, presenting mostly net positive charges at physiological pH (43). Considering their secondary structures, the AMPs may be classified as (i) linear α-helical peptides, (ii) α-helical peptides presenting a disulfide bridge in the C-terminal region, (iii) β-sheet peptides presenting disulfide bridges, (iv) cyclic peptides, and (v) peptides rich in a specific amino acid residue. The α-helical peptides generally do not present a well-defined secondary structure in aqueous medium but fold into amphiphilic α-helices in the presence of the hydrophobic environment of cell membranes along the helical axis (44).

The results showed that none of the fragments of the peptide MK58911-NH_2 showed anticryptococcal activity and toxicity to pulmonary fibroblasts (MRC5 cells) at the evaluated concentrations. Despite MK58911(4–11)-OH presenting a helix element of secondary structure, the peptide length does not seem to be enough to make this peptide active as an antifungal compound. The two other peptides [MK58911(1–7)-OH and MK58911(8–14)-NH_2] do not present anticryptococcal activity. These results suggest that some smaller fragments lack all or part of the helical element, which is required for antifungal activity. The removal of some residues from any of the termini apparently breaks the α-helical conformation necessary to promote the reported biological actions.

Regarding the comparison of the antifungal activities of MK58911-NH_2 and its derivative MH58911-NH_2, it was observed that the lysine-containing peptide was more potent than the histidine-containing one. This result may be related to the fact that at physiological pH (used in the assay), the peptide carrying lysine residues presents the Lys side chains protonated, while in the peptide carrying histidine residues, the His side chains (imidazole) are neutral at physiological pH. Thus, the polycationic nature of MK58911-NH_2 is more pronounced than that presented by MH58911-NH_2 at physiological pH, making the lysine peptide more active. Following the present findings, a previous study demonstrated that the replacement of all basic amino acids in the heparin-binding peptides ARK24 and AKK24 by histidines (AHH24:1 and AHH24:2) abrogates their antibacterial and antifungal activities (45). However, the derivative MH58911-NH_2 showed less toxicity in macrophages than MK58911-NH_2, demonstrating that the insertion of histidine residues is beneficial for this parameter. The histidine residues present reduced pK_a values compared to lysine residues; thus, despite maintaining polycationicity, the total replacement of lysine by histidine modifies the biophysical parameters of the molecule, which in turn causes the reduction of the toxicity of MH58911-NH_2 in macrophages.

We also evaluated the effect of MH58911-NH_2 on *C. neoformans* in macrophages and biofilms. We hypothesize that although this peptide had no action against *Cryptococcus* spp., the pH value at which histidines ionize (gaining a positive charge) is lower than the pH value at which lysines ionize. In this way, the more acidic medium of the interior of the macrophages could benefit MH58911-NH_2 activity, as demonstrated by a previous study with histidine-rich peptides (45). However, the peptide was unable to act on intramacrophage fungi. On the other hand, MH58911-NH_2 at higher

concentrations exhibited activity against *C. neoformans* in biofilms. Recent reviews (16, 46) demonstrated that some AMPs act against microorganisms in both planktonic and biofilm forms, such as MK58911-NH_2. Others do not demonstrate activity against planktonic cells but can act in biofilms by the rupture or alteration of extracellular matrix components, which is a possible mechanism of MH58911-NH_2.

In conclusion, the peptide MK58911-NH_2 did not promote damage to the cell wall and capsule of *C. neoformans* but reduced the number and size of fungal cells. In addition, it reduced the fungal burden of *C. neoformans* in macrophages and zebrafish embryos. It also acted on biofilm formation and mature biofilms of *C. neoformans*. A derivative peptide (MH58911-NH_2) in which the lysine residues of MK58911-NH_2 were replaced by histidine residues reduced the activity against extracellular and intracellular *C. neoformans*. On the other hand, it was active against biofilms, and it was beneficial in reducing toxicity in macrophages. In summary, the results *in vitro* and *in vivo* show that peptide MK58911-NH_2 can be a promising agent against cryptococcosis.

The present work opens a perspective for continuing peptide tests in mammalian models and verifying the antifungal activity and toxicity of other fragments and derivatives.

MATERIALS AND METHODS

Fungal strains. *C. neoformans* ATCC 90112 and *C. gattii* ATCC 56990 were purchased from the collection of the Laboratory of Clinical Mycology, Faculty of Pharmaceutical Sciences of UNESP, Araraquara, Brazil. *Cryptococcus* species were grown at 30°C for 48 to 72 h in Sabouraud dextrose agar.

Peptides. The peptides were synthesized under a solid phase using an automatic synthesizer (Prelude model; Protein Technologies Inc., USA), based on a 9-fluorenylmethoxy carbonyl (Fmoc) strategy, with the *N*-9-fluorenylmethoxy carbonyl reagent. The peptides were synthesized using 100 mg of NovaSyn TGR resin, with a degree of substitution of 0.2 mmol/g. In each cycle of synthesis, Fmoc-amino acid-OH (Novabiochem), containing *N*-hydroxybenzotriazole (HOBt·H_2O; Novabiochem) and *N*-methylmorpholine (NNM; Aldrich), was added as the amino acid-activating agent, and benzotriazol-1-1-hexafluorophosphate-oxy-Tris-pyrrolidine-phosphonium (PyBOP; Novabiochem) was added as a coupling agent, for 30 min. After each coupling cycle, five washes of the resin were performed with *N*,*N*-dimethylformamide (DMF; Sigma). Fmoc removal was performed using 30% (vol/vol) piperidine (Sigma) in DMF. All reactions were performed under mechanical agitation in a safety chapel. After coupling the last amino acid residue, the resin was washed with methanol (Mallinckrodt) and dried in a lyophilizer (model MLW-LGA 05; Heto). After drying, cleavage between the peptide and resin was performed using a solution containing 82.5% (vol/vol) trifluoroacetic acid (TFA; Mallinckrodt), 5% (vol/vol) anisole (Sigma), 2.5% (vol/vol) ethanedithiol (Aldrich), 5% (mass/vol) phenol, and 5% (vol/vol) ultrapure water for 2 h under mechanical stirring. This TFA-anisol-ethanedithiol-phenol-peptide solution was filtered to remove the resin and centrifuged at 4°C (model 5810R; Eppendorf) for 15 min at 3,000 rpm in the presence of ethyl ether (Synth). The sedimented material was then resuspended in ultrapure MilliQ Advantage A10 water (Millipore) and purified by reverse-phase high-performance liquid chromatography (RP-HPLC). The quality control for the peptides was done by electrospray ionization-mass spectrometry (ESI-MS) analysis.

The mastoparan analog peptide MK58911-NH_2 (MK) was previously engineered and used as a structural model for the design of other analog peptides (19). Three fragments of the peptide MK58911-NH_2 were also synthesized: MK58911(1–7)-OH (the C-terminal half), MK58911(8–14)-NH_2 (the N-terminal half), and MK58911(4–11)-OH (the central portion) (Table 1). Furthermore, an analog peptide of MK58911-NH_2 was synthesized in which all the lysine residues were replaced by histidine residues (MH58911-NH_2). Fresh aqueous solutions in sterile water were prepared for all peptides to be used in the bioassays.

Simulation of the secondary structures of peptides. The sequences of the five peptides were loaded into the dialog box of the PEP2D algorithm (https://webs.iiitd.edu.in/raghava/pep2d/submit.html) (26) and submitted to estimate the occurrence of elements of secondary structures using the RandomForest classifier approach, which calculates the probabilistic values of the helices, sheets, and coils. Next, values are optimized using weights, and finally, the probability of each element of the secondary structure is assigned. The results were shown in a table format, exhibiting the percentage of each element of secondary structure and a graphic representation of the secondary structures for each peptide.

Cell wall and fungal cell counts. *C. neoformans* colonies were dissolved in phosphate-buffered saline (PBS) and diluted in a solution containing RPMI 1640 culture medium, 0.165 M morpholinepropanesulfonic acid (MOPS) (pH 7.4), L-glutamine, and 2% glucose to obtain 1×10^6 cells/ml. One hundred microliters of this fungal suspension was added to a 96-well plate. Subsequently, 100 μl of MK58911-NH_2 (15.625 μg/ml [1/2× MIC], 31.25 μg/ml [MIC], and 62.50 μg/ml [2× MIC]), amphotericin B (0.125 μg/ml [MIC]), and fluconazole (1 μg/ml [MIC]), all diluted in RPMI 1640 medium, was added to the plate. The fungal suspension and RPMI 1640 medium were used as the positive and negative controls, respectively. The plate was incubated at 37°C at 150 rpm for 4 h. After that, 10 μl of calcofluor white was added to reach a 50-μg/ml concentration, and the mixture was incubated for 5 min at room temperature. The samples were centrifuged at 3,500 rpm for 5 min (5810R centrifuge; Eppendorf) and washed with PBS. Next, 200 μl of PBS was added to each well, and the images were acquired with an In Cell Analyzer 2000 microscope (GE). The quantification of the

average fluorescence intensity per cell to verify the action of the peptide on the chitin content present in the cell wall and the fungal cell count were performed by using In Cell Investigator software. Three independent experiments were performed.

Cellular and capsule sizes. The *C. neoformans* suspension and treatment preparation with the MK58911-NH_2 peptide were carried out as described above for the cell wall assay. After 4 h, fungal cells were centrifuged and washed with PBS. A sample from each group (control and MK) was suspended in India ink, and images were acquired in a Primovert inverted microscope (Carl Zeiss). Cellular and capsular sizes of parent cells were measured using ImageJ software. Another sample from each group was incubated with 10 μg/ml of capsule-binding mouse monoclonal antibody 18b7 at 37°C at 150 rpm for 1 h. Subsequently, 1 μl of anti-mouse IgG-FITC was added, and the samples were incubated at 37°C at 150 rpm for 30 min. The images were acquired with an In Cell Analyzer 2000 microscope (GE). The quantification of the average fluorescence intensity per cell to verify the action of the peptide on the capsule was performed with In Cell Investigator software. Three independent experiments were performed.

Zebrafish infected with *C. neoformans*. A zebrafish embryo infection model by immersion was used, as previously described for *C. albicans*, with some modifications (22). The housing and breeding of the fish used in this study received appropriate institutional approvals (permit number 01.0082.2014). Briefly, 15 zebrafish embryos at 24 h postfertilization (hpf) and cultured in embryo medium at 28°C were used. Embryos were coincubated in wells with *C. neoformans* at 1×10^6 cells/ml by immersion. The plate was incubated at 28°C at 80 rpm for 24 h. Subsequently, the embryos were washed twice with embryo medium and transferred to a 96-well plate (1 embryo/well). Next, 100 μl of MK58911-NH_2, amphotericin B, and fluconazole, all diluted in embryo medium and at the MIC, was added to the wells. The plate was incubated at 28°C at 80 rpm for 24 h. After that, the embryos were lysed individually in 2% Triton X-100–PBS using a 26-gauge needle. A 1-fold dilution was performed in PBS, and 10 μl was plated onto Sabouraud dextrose agar containing 50 mg/liter chloramphenicol. The plates were incubated at 37°C for 48 to 72 h, and CFU were determined. The groups were tested in triplicate, and two independent experiments were performed. Images of some embryos 4 h after infection with *C. neoformans*, labeled with calcofluor white, were acquired with an In Cell Analyzer 2000 microscope (GE).

Antifungal activity. Anti-*Cryptococcus* activity was determined by the broth microdilution method according to document M27-A3 from the Clinical and Laboratory Standards Institute (47). Briefly, 100 μl of a fungal suspension at 1×10^6 to 5×10^6 cells/ml in RPMI 1640 medium was added to each well of the 96-well plate. Subsequently, 100 μl of MK58911-NH_2, MK58911(1–7)-OH, MK58911(8–14)-NH_2, MK58911(4–11)-OH, and MH58911 (0.48 to 250 μg/ml); amphotericin B (0.016 to 8 μg/ml); and fluconazole (0.063 to 32 μg/ml), all diluted in RPMI 1640 medium, was added to the plate. The fungal suspension and RPMI 1640 medium were used as the positive and negative controls, respectively. The plate was incubated at 37°C at 150 rpm for 48 h. Next, fungal growth was visually observed, and the MIC was determined. Three independent experiments were performed.

Cytotoxicity. The impact of peptides on the viability of pulmonary fibroblasts (MRC5) was also evaluated. Cells were cultured in Dulbecco's high-glucose modified Eagle medium (DMEM; Gibco, Thermo Fisher Scientific) supplemented with 10% fetal bovine serum (FBS) in 25-cm^2 flasks. For the assay, cells were seeded into 96-well plates at 5×10^4 cells/well. The cells were left to grow at 37°C in a 5% CO_2 incubator for 24 h until they reached confluence. Medium from the wells was then aspirated, and 100 μl of the MK58911-NH_2, MK58911(1–7)-OH, MK58911(8–14)-NH_2, MK58911(4–11)-OH, and MH58911-NH_2 (0.48 to 250 μg/ml), all diluted in DMEM, was added to the plate. DMEM and dimethyl sulfoxide (DMSO) were used as the positive and negative controls, respectively. The plates were then incubated at 37°C in a 5% CO_2 incubator for 24 h. Resazurin (0.01%; Sigma-Aldrich) was then used to assess the viability of the cells according to the manufacturer's instructions. After 4 h of incubation at 37°C in a 5% CO_2 incubator, the fluorescence intensity was measured using a microplate reader (BioTek) at 570 to 600 nm. The fluorescence values were normalized by the positive control and expressed as a percentage of metabolic activity. Values for the 50% inhibitory concentration (IC_{50}) were calculated. Three independent experiments were performed.

Intramacrophage activity. The infection assay of *Cryptococcus* in J774 macrophages was performed according to methods described in a previous study (48), with some modifications. Macrophages (5×10^5 cells/ml) were seeded into a 96-well plate in DMEM supplemented with 10% FBS at 37°C in 5% CO_2. After 18 to 24 h, they were activated for 1 h with 150 ng/ml phorbol 12-myristate 13-acetate (PMA; Sigma-Aldrich) in serum-free DMEM (SF-DMEM). During that time, 1×10^6 cells/ml of *C. neoformans* were opsonized with mouse monoclonal antibody 18b7. Next, macrophages were infected with opsonized fungal cells (multiplicity of infection [MOI] of 5:1) for 2 h at 37°C with 5% CO_2. After that, the macrophages were washed 4 times with PBS. The supernatant was discarded, and 100 μl of the solutions of MK58911-NH_2, MH58911-NH_2, amphotericin B, and fluconazole, all diluted in SF-DMEM and at the MIC, was added to the plate. The medium was used as a positive control. The plate was incubated at 37°C in 5% CO_2 for 24 h. Subsequently, the macrophages were lysed using sterile water for 30 min at 37°C. An aliquot (10 μl) of the 2-fold dilution in PBS was plated onto Sabouraud dextrose agar. The plates were incubated at 37°C for 48 to 72 h, and the CFU were determined. Three independent experiments were performed. The impact of peptides on the viability of macrophages (J774) was also evaluated as described above for MRC5 cells.

Antibiofilm activity. The biofilm formation of *C. neoformans* and the activity of MK58911-NH_2 and MH58911-NH_2 were evaluated according to methods described previously (13), with slight modifications. Briefly, *C. neoformans* was grown in Sabouraud dextrose broth at 30°C at 150 rpm for 24 h. To evaluate the effect of peptides on biofilm formation, a fungal suspension of 1×10^7 cells/ml in minimal medium (20 mg/ml thiamine, 30 mM glucose, 26 mM glycine, 20 mM $MgSO_4 \cdot 7H_2O$, 58.8 mM KH_2PO_4) was

prepared, and 100 μl of the suspension was added to individual wells of 96-well polystyrene plates (TPP, Switzerland). Subsequently, 100 μl of MK58911-NH_2, MH58911-NH_2 (31.25 to 1,000 μg/ml), amphotericin B (0.25 to 8 μg/ml), or fluconazole (1 to 32 μg/ml), all diluted in minimal medium, was added to the wells. The plate was incubated at 37°C for 48 h. To evaluate the effect of the peptides on the mature biofilm, 100 μl of the fungal suspension was added to individual wells of a 96-well plate, and the plate was incubated at 37°C for 48 h. After that period, the supernatant was removed, and the peptides and drugs were added. The plate was again incubated at 37°C for 48 h. The metabolic activity of the biofilms was quantified by the 2,3-bis(2-methoxy-4-nitro-5-sulfophenyl)-5-[(phenylamino)carbonyl]-2*H*-tetrazolium hydroxide (XTT) reduction assay. For this, a solution with 50 μl of XTT (1 mg/ml in PBS) and 4 μl of menadione (1 mM in ethanol; Sigma-Aldrich, São Paulo, SP, Brazil) was added to each well of the 96-well plate. After 3 h of incubation at 37°C, the fluorescence intensity was measured using a microplate reader (BioTek) at 490 nm. Subsequently, the percentage of metabolic activity of the biofilm treated with peptides/drugs was compared to that of the untreated control. Three independent experiments were performed.

Statistical analysis. Graphs and statistical analyses were performed using GraphPad Prism 5.0 (GraphPad Software Inc., La Jolla, CA). The data for the cell wall, fungal cell counts, and CFU (zebrafish and macrophage) were compared using one-way analysis of variance (ANOVA) followed by Dunnett's correction. The data for cellular and capsule sizes were compared by a *t* test. *P* values of <0.05 were considered significant.

ACKNOWLEDGMENTS

We thank Robin May for generous support and critical comments on the manuscript. We thank Patricia Albuquerque for kindly providing the 18b7 antibody. We also thank Claudia Tavares dos Santos for technical support in the acquisition of images.

This work was supported by the Conselho Nacional de Pesquisa e Desenvolvimento (CNPq), the Fundação de Amparo à Pesquisa do Estado de São Paulo (FAPESP) (grant numbers 2017/06658-9 and 2016/16212-5), and the Coordenação de Aperfeiçoamento de Pessoal de Nível Superior-Brasil (CAPES) (Finance Code 001).

REFERENCES

1. Rajasingham R, Smith RM, Park BJ, Jarvis JN, Govender NP, Chiller TM, Denning DW, Loyse A, Boulware DR. 2017. Global burden of disease of HIV-associated cryptococcal meningitis: an updated analysis. Lancet Infect Dis 17:873–881. https://doi.org/10.1016/S1473-3099(17)30243-8.
2. Del Poeta M, Casadevall A. 2012. Ten challenges on Cryptococcus and cryptococcosis. Mycopathologia 173:303–310. https://doi.org/10.1007/s11046-011-9473-z.
3. Alvarez M, Casadevall A. 2006. Phagosome extrusion and host-cell survival after Cryptococcus neoformans phagocytosis by macrophages. Curr Biol 16:2161–2165. https://doi.org/10.1016/j.cub.2006.09.061.
4. Ma H, Croudace JE, Lammas DA, May RC. 2006. Expulsion of live pathogenic yeast by macrophages. Curr Biol 16:2156–2160. https://doi.org/10.1016/j.cub.2006.09.032.
5. Johnston SA, May RC. 2013. Cryptococcus interactions with macrophages: evasion and manipulation of the phagosome by a fungal pathogen. Cell Microbiol 15:403–411. https://doi.org/10.1111/cmi.12067.
6. Park BJ, Wannemuehler KA, Marston BJ, Govender N, Pappas PG, Chiller TM. 2009. Estimation of the current global burden of cryptococcal meningitis among persons living with HIV/AIDS. AIDS 23:525–530. https://doi.org/10.1097/QAD.0b013e328322ffac.
7. Kozic H, Riggs K, Ringpfeil F, Lee JB. 2008. Disseminated Cryptococcus neoformans after treatment with infliximab for rheumatoid arthritis. J Am Acad Dermatol 58:S95–S96. https://doi.org/10.1016/j.jaad.2006.12.015.
8. Neofytos D, Fishman JA, Horn D, Anaissie E, Chang C-H, Olyaei A, Pfaller M, Steinbach WJ, Webster KM, Marr KA. 2010. Epidemiology and outcome of invasive fungal infections in solid organ transplant recipients. Transpl Infect Dis 12:220–229. https://doi.org/10.1111/j.1399-3062.2010.00492.x.
9. Mourad A, Perfect JR. 2018. The war on cryptococcosis: a review of the antifungal arsenal. Mem Inst Oswaldo Cruz 113:e170391. https://doi.org/10.1590/0074-02760170391.
10. Nett JE, Andes DR. 2016. Antifungal agents: spectrum of activity, pharmacology, and clinical indications. Infect Dis Clin North Am 30:51–83. https://doi.org/10.1016/j.idc.2015.10.012.
11. Pfaller MA. 2012. Antifungal drug resistance: mechanisms, epidemiology, and consequences for treatment. Am J Med 125:S3–S13. https://doi.org/10.1016/j.amjmed.2011.11.001.
12. Arastehfar A, Gabaldon T, Garcia-Rubio R, Jenks JD, Hoenigl M, Salzer HJF, Ilkit M, Lass-Florl C, Perlin DS. 2020. Drug-resistant fungi: an emerging challenge threatening our limited antifungal armamentarium. Antibiotics (Basel) 9:877. https://doi.org/10.3390/antibiotics9120877.
13. Martinez LR, Casadevall A. 2006. Susceptibility of Cryptococcus neoformans biofilms to antifungal agents in vitro. Antimicrob Agents Chemother 50:1021–1033. https://doi.org/10.1128/AAC.50.3.1021-1033.2006.
14. da Costa JP, Cova M, Ferreira R, Vitorino R. 2015. Antimicrobial peptides: an alternative for innovative medicines? Appl Microbiol Biotechnol 99:2023–2040. https://doi.org/10.1007/s00253-015-6375-x.
15. Buda De Cesare G, Cristy SA, Garsin DA, Lorenz MC. 2020. Antimicrobial peptides: a new frontier in antifungal therapy. mBio 11:e02123-20. https://doi.org/10.1128/mBio.02123-20.
16. Yasir M, Willcox MDP, Dutta D. 2018. Action of antimicrobial peptides against bacterial biofilms. Materials (Basel) 11:2468. https://doi.org/10.3390/ma11122468.
17. Batoni G, Maisetta G, Esin S. 2016. Antimicrobial peptides and their interaction with biofilms of medically relevant bacteria. Biochim Biophys Acta 1858:1044–1060. https://doi.org/10.1016/j.bbamem.2015.10.013.
18. da Silva AV, De Souza BM, Dos Santos Cabrera MP, Dias NB, Gomes PC, Neto JR, Stabeli RG, Palma MS. 2014. The effects of the C-terminal amidation of mastoparans on their biological actions and interactions with membrane-mimetic systems. Biochim Biophys Acta 1838:2357–2368. https://doi.org/10.1016/j.bbamem.2014.06.012.
19. Souza BM, Cabrera MP, Gomes PC, Dias NB, Stabeli RG, Leite NB, Neto JR, Palma MS. 2015. Structure-activity relationship of mastoparan analogs: effects of the number and positioning of Lys residues on secondary structure, interaction with membrane-mimetic systems and biological activity. Peptides 72:164–174. https://doi.org/10.1016/j.peptides.2015.04.021.
20. Singulani JL, Galeane MC, Ramos MD, Gomes PC, Dos Santos CT, de Souza BM, Palma MS, Fusco Almeida AM, Mendes Giannini MJS. 2019. Antifungal activity, toxicity, and membranolytic action of a mastoparan analog peptide. Front Cell Infect Microbiol 9:419. https://doi.org/10.3389/fcimb.2019.00419.
21. Panzica-Kelly JM, Zhang CX, Augustine-Rauch K. 2012. Zebrafish embryo developmental toxicology assay. Methods Mol Biol 889:25–50. https://doi.org/10.1007/978-1-61779-867-2_4.
22. Chen YZ, Yang YL, Chu WL, You MS, Lo HJ. 2015. Zebrafish egg infection model for studying Candida albicans adhesion factors. PLoS One 10:e0143048. https://doi.org/10.1371/journal.pone.0143048.

23. Bojarczuk A, Miller KA, Hotham R, Lewis A, Ogryzko NV, Kamuyango AA, Frost H, Gibson RH, Stillman E, May RC, Renshaw SA, Johnston SA. 2016. Cryptococcus neoformans intracellular proliferation and capsule size determines early macrophage control of infection. Sci Rep 6:21489. https://doi.org/10.1038/srep21489.
24. Tenor JL, Oehlers SH, Yang JL, Tobin DM, Perfect JR. 2015. Live imaging of host-parasite interactions in a zebrafish infection model reveals cryptococcal determinants of virulence and central nervous system invasion. mBio 6:e01425-15. https://doi.org/10.1128/mBio.01425-15.
25. Davis JM, Huang M, Botts MR, Hull CM, Huttenlocher A. 2016. A zebrafish model of cryptococcal infection reveals roles for macrophages, endothelial cells, and neutrophils in the establishment and control of sustained fungemia. Infect Immun 84:3047–3062. https://doi.org/10.1128/IAI.00506-16.
26. Singh H, Singh S, Singh Raghava GP. 2019. Peptide secondary structure prediction using evolutionary information. bioRxiv https://doi.org/10.1101/558791.
27. Wang G, Li X, Wang Z. 2016. APD3: the antimicrobial peptide database as a tool for research and education. Nucleic Acids Res 44:D1087–D1093. https://doi.org/10.1093/nar/gkv1278.
28. Struyfs C, Cammue BPA, Thevissen K. 2021. Membrane-interacting antifungal peptides. Front Cell Dev Biol 9:649875. https://doi.org/10.3389/fcell.2021.649875.
29. Wang ZA, Li LX, Doering TL. 2018. Unraveling synthesis of the cryptococcal cell wall and capsule. Glycobiology 28:719–730. https://doi.org/10.1093/glycob/cwy030.
30. O'Meara TR, Alspaugh JA. 2012. The Cryptococcus neoformans capsule: a sword and a shield. Clin Microbiol Rev 25:387–408. https://doi.org/10.1128/CMR.00001-12.
31. Bose I, Reese AJ, Ory JJ, Janbon G, Doering TL. 2003. A yeast under cover: the capsule of Cryptococcus neoformans. Eukaryot Cell 2:655–663. https://doi.org/10.1128/EC.2.4.655-663.2003.
32. McClelland EE, Bernhardt P, Casadevall A. 2006. Estimating the relative contributions of virulence factors for pathogenic microbes. Infect Immun 74:1500–1504. https://doi.org/10.1128/IAI.74.3.1500-1504.2006.
33. Casadevall A, Steenbergen JN, Nosanchuk JD. 2003. 'Ready made' virulence and 'dual use' virulence factors in pathogenic environmental fungi—the Cryptococcus neoformans paradigm. Curr Opin Microbiol 6:332–337. https://doi.org/10.1016/s1369-5274(03)00082-1.
34. Bryan RA, Zaragoza O, Zhang T, Ortiz G, Casadevall A, Dadachova E. 2005. Radiological studies reveal radial differences in the architecture of the polysaccharide capsule of Cryptococcus neoformans. Eukaryot Cell 4:465–475. https://doi.org/10.1128/EC.4.2.465-475.2005.
35. Neto JB, da Silva CR, Neta MA, Campos RS, Siebra JT, Silva RA, Gaspar DM, Magalhaes HI, de Moraes MO, Lobo MD, Grangeiro TB, Carvalho TS, Diogo EB, da Silva Junior EN, Rodrigues FA, Cavalcanti BC, Junior HV. 2014. Antifungal activity of naphthoquinoidal compounds in vitro against fluconazole-resistant strains of different Candida species: a special emphasis on mechanisms of action on Candida tropicalis. PLoS One 9:e93698. https://doi.org/10.1371/journal.pone.0093698.
36. Cho J, Choi H, Lee J, Kim MS, Sohn HY, Lee DG. 2013. The antifungal activity and membrane-disruptive action of dioscin extracted from Dioscorea nipponica. Biochim Biophys Acta 1828:1153–1158. https://doi.org/10.1016/j.bbamem.2012.12.010.
37. Bechinger B. 1999. The structure, dynamics and orientation of antimicrobial peptides in membranes by multidimensional solid-state NMR spectroscopy. Biochim Biophys Acta 1462:157–183. https://doi.org/10.1016/S0005-2736(99)00205-9.
38. Samantaray S, Correia JN, Garelnabi M, Voelz K, May RC, Hall RA. 2016. Novel cell-based in vitro screen to identify small-molecule inhibitors against intracellular replication of Cryptococcus neoformans in macrophages. Int J Antimicrob Agents 48:69–77. https://doi.org/10.1016/j.ijantimicag.2016.04.018.
39. Ramage G, Rajendran R, Sherry L, Williams C. 2012. Fungal biofilm resistance. Int J Microbiol 2012:528521. https://doi.org/10.1155/2012/528521.
40. Pierce CG, Uppuluri P, Tristan AR, Wormley FL, Jr, Mowat E, Ramage G, Lopez-Ribot JL. 2008. A simple and reproducible 96-well plate-based method for the formation of fungal biofilms and its application to antifungal susceptibility testing. Nat Protoc 3:1494–1500. https://doi.org/10.1038/nprot.2008.141.
41. Wang K, Yan J, Dang W, Xie J, Yan B, Yan W, Sun M, Zhang B, Ma M, Zhao Y, Jia F, Zhu R, Chen W, Wang R. 2014. Dual antifungal properties of cationic antimicrobial peptides polybia-MPI: membrane integrity disruption and inhibition of biofilm formation. Peptides 56:22–29. https://doi.org/10.1016/j.peptides.2014.03.005.
42. Wang SH, Chen CC, Lee CH, Chen XA, Chang TY, Cheng YC, Young JJ, Lu JJ. 2020. Fungicidal and anti-biofilm activities of trimethylchitosan-stabilized silver nanoparticles against Candida species in zebrafish embryos. Int J Biol Macromol 143:724–731. https://doi.org/10.1016/j.ijbiomac.2019.10.002.
43. Mookherjee N, Anderson MA, Haagsman HP, Davidson DJ. 2020. Antimicrobial host defence peptides: functions and clinical potential. Nat Rev Drug Discov 19:311–332. https://doi.org/10.1038/s41573-019-0058-8.
44. Hollmann A, Martinez M, Maturana P, Semorile LC, Maffia PC. 2018. Antimicrobial peptides: interaction with model and biological membranes and synergism with chemical antibiotics. Front Chem 6:204. https://doi.org/10.3389/fchem.2018.00204.
45. Kacprzyk L, Rydengard V, Morgelin M, Davoudi M, Pasupuleti M, Malmsten M, Schmidtchen A. 2007. Antimicrobial activity of histidine-rich peptides is dependent on acidic conditions. Biochim Biophys Acta 1768:2667–2680. https://doi.org/10.1016/j.bbamem.2007.06.020.
46. Oshiro KGN, Rodrigues G, Monges BED, Cardoso MH, Franco OL. 2019. Bioactive peptides against fungal biofilms. Front Microbiol 10:2169. https://doi.org/10.3389/fmicb.2019.02169.
47. Clinical and Laboratory Standards Institute. 2008. Reference method for broth dilution antifungal susceptibility testing of yeasts; approved standard, 3rd ed. CLSI document M27-A3. Clinical and Laboratory Standards Institute, Wayne, PA.
48. Bielska E, Sisquella MA, Aldeieg M, Birch C, O'Donoghue EJ, May RC. 2018. Pathogen-derived extracellular vesicles mediate virulence in the fatal human pathogen Cryptococcus gattii. Nat Commun 9:1556. https://doi.org/10.1038/s41467-018-03991-6.